A Pulse generator based on Transmission line Transformer for Insulation Aging Test

Xiao Yu, Khanh-Hung Nguyen, Peter Zacharias
UNIVERSITY OF KASSEL
Wilhelmshoeher Allee 71
D-34121 Kassel, Germany
Phone: +49 (561) 804-6477
Email: Xiao.yu@uni-kassel.de
URL: http://www.uni-kassel.de

July 11, 2022

Acknowledgments

Keywords

Abstract

A pulse generator consisting of a transmission line transformer and GaN-based full bridge for generating high-repetitive impulse voltage stress with a high slew rate is proposed. GaN-half-bridges are used to generate fast switching edges, while the wide-band transmission line transformer is adopted to achieve the required voltage gain for an accelerated test without losing the interested high-frequency components contained in the fast edges. Another benefit of using the transmission line transformer is the spatial separation of pulse generation at room temperature and devices under test in a climate chamber, where the temperature for an accelerated test can be up to 150°C. The detailed operation principle, design considerations, simulation implementation, and experimental results for the proposed pulse generator are also presented. A peak-to-peak voltage of $400V \times 8$ and a maximal voltage slew rate of 250 V/ns have been achieved.

Introduction

New semiconductor technologies (e.g., 650 V GaN HEMTs) can generate high dv/dt during switching operations, resulting in significantly higher stress than that of conventional setups [1]. Together with high repetition rates, this stress can damage the insulation material and lead to partial discharges and breakdown. To generate the desired impulse voltage stress for the investigation of the long-term stability of relevant insulation materials under real geometries and environmental conditions, a pulse generator is needed, which should be able to provide a high charging/discharging current to the devices under test (DUTs) to achieve high dv/dt. On the other hand, for an accelerated lifetime test, the DUTs should be placed and stressed in a climate chamber, where the test temperature can be up to 150°C. No semiconductors can operate long hours under this ambient temperature. Therefore, the pulse generator should also enable a spatial separation between semiconductors generating the pulses and the DUTs. Furthermore, to fulfill a set of different test conditions, the slew rate, repetition rate, pulse width and amplitude of the generated voltage pulses should be easy and flexible to adjust.

In general, there are two basic methods for constructing pulse transformers, namely, ordinary transformers according to induction law and the transmission line type of transformer. The permeability drop and influences through stray capacitance and leakage inductance of windings limit the usage of ordinary transformers in the high-frequency range [2] [3]. The transmission line transformer (TLT) was first introduced by Guanella in 1944, and C.L.Ruthroff made another significant work in 1959 [4]. Due to their wide bandwidth and simple structure, TLTs are widely used for impedance matching for antennas and wideband voltage amplifiers in the high frequency and very high-frequency range [5] [6] [7].

For these reasons, a transmission line transformer-based pulse generator has been proposed and developed in this work. GaN-half-bridges are used to generate fast switching edges close to the real application scenarios. They are also responsible for the adjustable voltage amplitude, pulse width and repetition rate. At the same time, the transmission line transformer is adopted to achieve the required voltage gain for an accelerated test without losing the important high-frequency components contained in the fast edges. In the meantime, coaxial cables with a non-standard and lower characteristic impedance of 25Ω are chosen for a higher capacitive charging/discharging current so a fast rising/falling edge. The PTFE dielectrics of these coaxes allow the line ends to be placed and work in the climate chamber under high temperatures. In this paper, the relevant concepts and operation principle of the transmission line transformer has been presented. To extend the upper and lower bandwidth limits, a combination of ferrite materials is used.

The operating principle of transmission line transformer

The steep rising and falling edges of pulses contain a spectrum of harmonics with different intensities. The highest frequencies in the spectrum are determined by the slope of the pulse edges and are not related to the repetition frequency of the pulse train. A rule-of-thumb formula can be used to estimate the upper-frequency limit:

$$f_r = \frac{1}{\pi \cdot min(t_r, t_f)} \tag{1}$$

Where t_r and t_f the rising time and falling time of a pulse, respectively.

The high-frequency effects become effective once the length of the transmission line approaches the order of magnitude of the wavelength of the highest frequency contained in the impulse spectrum [16]. Since the highest frequencies are still significantly higher than the upper-frequency limit f_r, the critical length l_{crit}, from which the line cannot be treated as electrically short, and the high-frequency effects should no longer be neglected, must therefore be significantly shorter than the wavelength λ corresponding to f_r:

$$\lambda = \frac{v}{f_r} = \frac{c \cdot \pi \cdot min(t_r, t_f)}{\sqrt{\varepsilon_r \mu_r}}, \ l_{crit} \approx \frac{\lambda}{10} \tag{2}$$

Where ε_r and μ_r are, respectively, the relative permittivity and permeability of a medium in which the wave propagates. In fact, disturbances like overshoots occur already below this critical length but would not cause dramatic consequences. By using the high-frequency effects, a special design of transformers can be realized for high frequencies and pulse applications. These transformers use the propagation characteristics of electromagnetic waves in lines and are therefore also called delay line transformers [9]. Different forms of transmission lines such as a double line, a coaxial cable, a twisted pair, or a pair of wires wound on a ferrite core. In this work, only coaxial cables are considered.
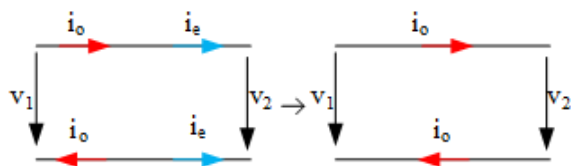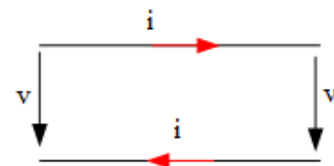

Fig. 1: Current Modes [3]   Fig. 2: Short line assumption

The following properties apply to an ideal TLT [3]:

- For a properly designed transmission line, only the current of the odd mode can flow through the line (see Fig. 1).
- All lines have the same length. The channels between two conductors of each line can be considered short compared to the intentionally delayed channels between conductors and the true ground.
- For a short line, the input voltage of a line is equal to its output voltage (see Fig. 2).
- Two different transmission lines are neither electrically nor magnetically coupled.
- The lines are connected in parallel on the input side and series on the output side (see Fig. 3).
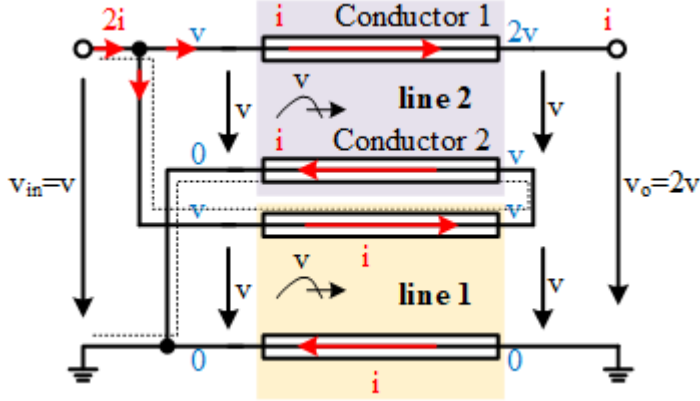- The order of a TLT is defined as the number of used lines.

Fig. 3: Ideal TLT of 2nd order [9]

(a) Series-Parallel-Termination
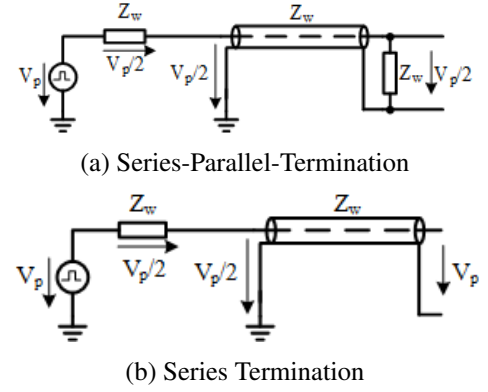
(b) Series Termination

Fig. 4: Impedance matching

As shown in Fig.3, the ideal voltage gain and impedance ratio can be derived as:

$$n = \frac{v_o}{v_{in}} = \frac{i_{in}}{i_o} = 2, \ R_{in} = \frac{v}{2i} = \frac{1}{4} \cdot \frac{2v}{i} = \frac{1}{4} R_o = \frac{1}{n^2} R_o \qquad (3)$$

The properly terminated transmission lines guarantee an undisturbed operation of TLT. Many methods are possible for a reflection-free termination (see Fig.4). The proposed pulse generator utilizes only the series termination, so in the case of a TLT with high order, no resistor needs to be dimensioned for the high output voltage. Furthermore, the incident voltage waves are totally reflected at the high impedance line ends due to a voltage reflection factor near +1 (capacitive load) and thus a voltage doubling occurs there and the voltage amplitude bounces back to V_p (see Fig. 4(b)). The reflected waves are eventually absorbed at the beginning of the line by the series resistor without causing further reflections.

Besides the propagation channels between the inner and outer conductor of the coaxial cables, the outer conductors and the ground form additional propagation channels, which prevent the normal operation of the transformer due to unwanted secondary reflections and short-circuit paths (see Fig.3 dot line) [10]. The transformer operates only when the secondary mode pulses are negligibly small, or be delayed a very long time, or both, without affecting the desired primary mode [2]. For these reasons, the usage of ferrite cores and ferrite sleeves is necessary. Due to the high permeability of the ferrites, the secondary mode pulses experience high impedance and larger delay in the channels between outer conductors and the ground plane. Another fact is that the highest frequency component in pulses can easily exceed 100 MHz, while the permeability of MnZn-ferrite (manganese zinc) drops rapidly from several megahertz. In order to provide enough impedance even in the high-frequency range, the cables are firstly wounded on the ferrite cores to obtain higher air inductance. Secondly, ferrite sleeves from NiZn (nickel-zinc) are installed on the coaxial cables, whose permeability is still far above zero in this frequency range (see Fig.5).

Compared to MnZn ferrites, the NiZn ferrites though have smaller permeability in the low-frequency range, but the feasible frequency range is much wider than that of MnZn ferrites and can be up to GHz-range. A combination of the two materials seems to be a good solution. It should be noted that, as shown in Fig.6, the higher the order of a cable, the higher the voltage stress on the installed ferrites so that the flux linkage. Therefore, the cables belonging to higher orders need more ferrites. In contrast, no ferrite
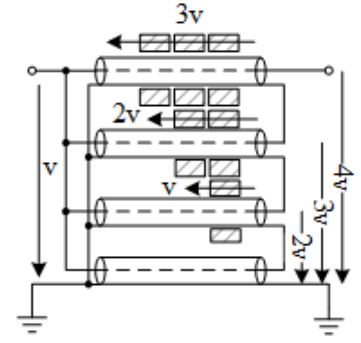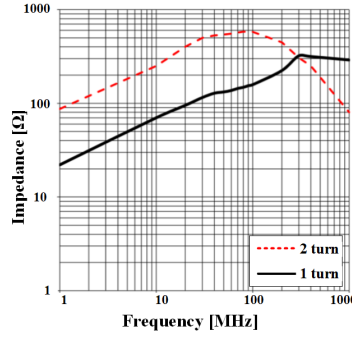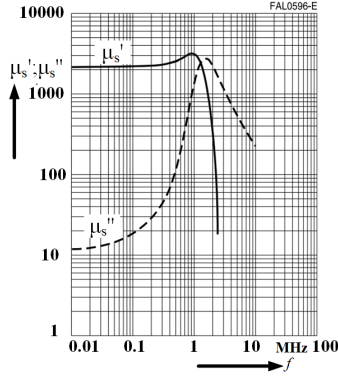
Fig. 5: Permeablitiy: MnZn (left) [11]; Impedance:NiZn (right) [12]

Fig. 6: Voltage on ferrites

is required for the cable at the bottom.

Basic circuit diagram and operation of proposed pulse generator

The pulse generator mainly consists of two GaN half-bridges, split DC link capacitors for blocking DC paths, resistors for impedance matching, and two TLTs of 4th order. The outer conductors of the bottom coaxial cable in each TLT are connected, while the DUT (device under test) is connected between two inner connectors of the top coaxial cable in each TLT. Fig. 7 shows the basic topology of the proposed pulse generator.
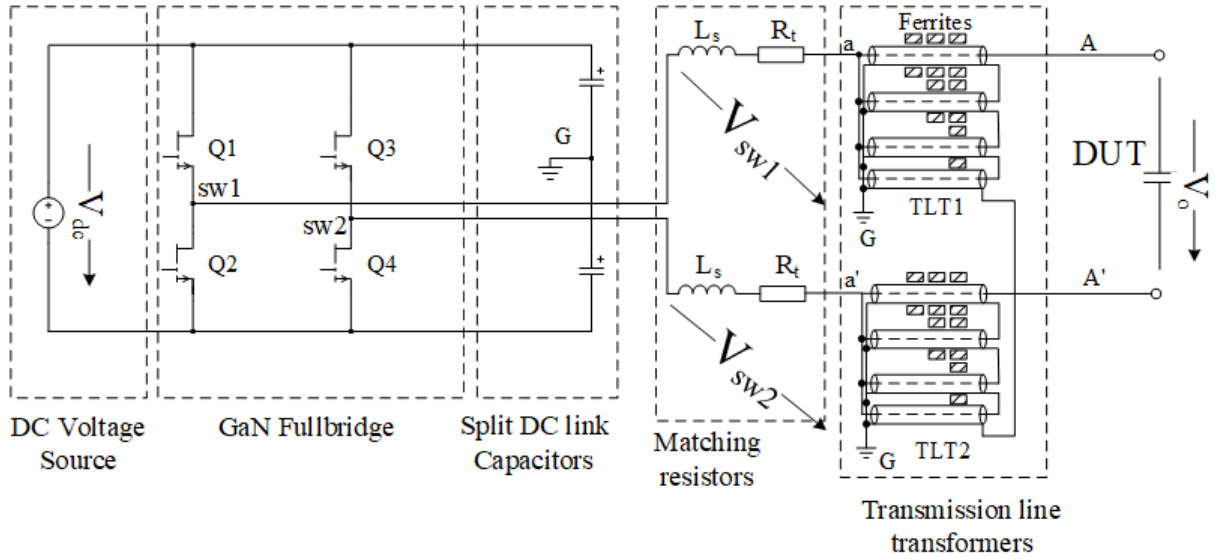

Fig. 7: Schematic of the proposed pulse generator

The relevant waveforms for the proposed pulse generator are shown in Fig.8. The GaN half-bridges generate complementary voltage pulses, V_{sw1} and V_{sw2}, with amplitude of $V_p = V_{dc}/2$. Taking the operation of TLT1 in Fig.7 as an example, since the matching resistors and the input impedance of TLT1 form a voltage divider, the amplitude of the incident voltage wave into the TLT1 is half of the pulse amplitude (see Fig.4). As the cables are parallel connected on the input side, a voltage wave with an amplitude of $V_p/2$ starts to travel between each cable's inner and outer conductor and towards the line end. Due to the same cable length, these voltage waves reach the serial connected line ends simultaneously. An Amplitude of $nV_p/2$ is induced at the output of TLT1. Taking the total reflection at the high impedance line ends into account, the amplitude of TLT1 output voltage V_{AG} equals nV_p. This also applies analogously to

the wave propagation in TLT2, which results in an output voltage $V_{A'G}$ with an amplitude of $-nV_p$. Consequently, the amplitude of the voltage across the DUT equals the potential difference between two top inner conductors, which corresponds to $2nV_p$. The maximal change in voltage equals $4nV_p$, which occurs at the falling edge from $2nV_p$ to $-2nV_p$. It is noteworthy that to avoid shoot-through in half-bridges, a dead time t_d is inserted. During the dead time, because both switches in one half-bridge are open, exists no discharging path for charged cables, so the bridge voltages v_{sw1} and v_{sw2} are clamped. These voltages are allowed to change only when one switch in the corresponding half-bridge is on. Therefore, the dead time will not affect the output waveform.
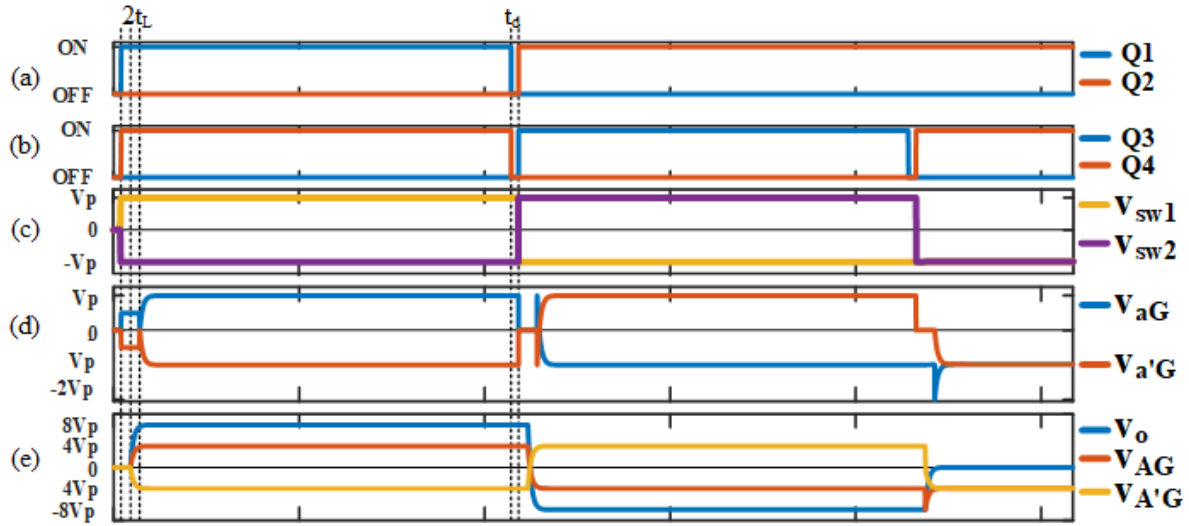

Fig. 8: Typical waveforms from simulation: (a), (b) Conductivity of switches ; (c) complementary voltage pulses ; (d) input voltages of TLTs ; (e) output voltage of each TLT and the voltage across the DUT

Simulation

The simulation model of the transmission line has been developed in [13]. For a lossless line, its two-port equations are derived as follows:

$$i_a(t) = \frac{1}{Z_w}v_a(t) - i_a(t - t_L), \ i_a(t - t_L) := \frac{1}{Z_w}v_e(t - t_L) - i_e(t - t_L)$$
$$i_e(t) = \frac{1}{Z_w}v_e(t) - i_e(t - t_L), \ i_e(t - t_L) := \frac{1}{Z_w}v_a(t - t_L) - i_a(t - t_L)$$

(4)

Where i_a and i_e the current flows into the line beginning and the line end, respectively, v_a and v_e the voltage across the input and output port of the transmission line, respectively. For a lossless line, applies:

$$Z_w = \sqrt{\frac{L'}{C'}} \ (real), \ \nu = \frac{1}{\sqrt{L'C'}}$$

(5)

It is assumed that the length of the line is equal to l. Then, the time for a voltage wave propagating from line beginning to the line end is:

$$t_L = \frac{l}{\nu} = \frac{l}{\sqrt{L'C'}}$$

(6)

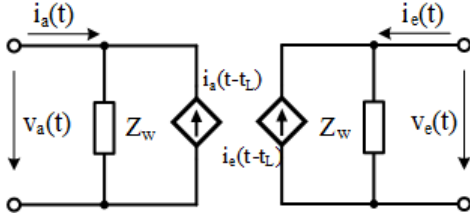Eq. 4 can be represented by the following equivalent circuit:

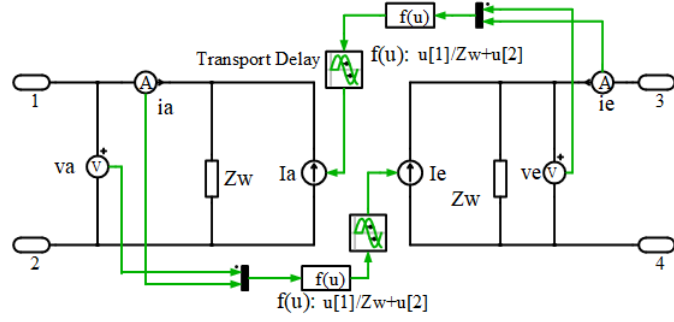Fig. 9: Equivalent circuit for a lossless transmission line [13]

Fig. 10: Simulation realization of the model in PLECS

Specifications and design considerations

The required voltage slew rate range is from 100 to 250 V/ns, and a maximal peak-to-peak output voltage of 400 V×8 is prescribed for an accelerated aging test.

GaN full-bridge

GaN-HEMT transistors have smaller $R_{ds(on)}$ and need much fewer gate charges Q_G, which leads to a faster switching transient [1] and is beneficial for the generation of fast pulse edges. Commercial evaluation boards of GaN half-bridge offer high reliability, which also reduces the time consumption for designing gate driver and PCB layout of the full-bridge. Considering the limited project duration, the half-bridge evaluation board GS66508T-EVBDB2 from GaN-System has been chosen. The disadvantages of using evaluation boards are the fixed gate resistance and PCB layout of the bridges. It is worth mentioning that the method adopted in this work for adjusting the voltage slew rate is by introducing different loop inductance L_s (see Fig.7) instead of a changeable gate resistance through a potentiometer. However, the minimal achievable loop inductance $L_{s,min}$ so that the highest slew rate cannot be further reduced due to the fixed PCB layout of the evaluation board. For a well-designed and application-oriented GaN-full-bridge with changeable gate resistance, steeper edges, and more flexible adjustment of the slew rate are possible.

The operating voltage of the chosen GS66508T has been limited to 400 V for reliability reasons though a voltage rating of 650 V. To achieve the desired maximal voltage slew rate, the relation in Eq. 7 must be fulfilled:

$$\frac{\mathrm{d}v_o}{\mathrm{d}t}\Big|_{max} \approx \frac{\Delta V_{o,max}}{\tau_o} = \frac{4n\frac{400V}{2}}{2n \times 10^{-3}\frac{Z_w}{[\Omega]}\frac{C_{DUT}}{[pF]} \cdot ns} \geq 250\frac{V}{ns} \tag{7}$$

Where τ_o is the time constant of the output equivalent circuit, Z_w the surge impedance of the chosen coaxial cable, and C_{DUT} the capacitance of paralleled twisted pairs to be tested. The maximal allowable capacitance of DUTs can be derived as $C_{DUT,max} = 64pF$ for 25-Ω-coax. Taking the rising and falling time of V_{sw1} and V_{sw2}, which are decided by the switching speed of GaN switches, the matching resistance R_t and the loop inductance L_s, and the pulse droop due to finite secondary impedance into consideration, the total capacitance of paralleled DUTs should be lower than 64 pF. It is worth mentioning that the slew rate is theoretically independent of the order n, and TLTs are used to achieve the required peak-to-peak voltage.

Coaxial Cable

The desired voltage slew rate is mainly decided by loop inductance, the characteristic impedance of the cable, and the capacitance of DUT. The coaxial cables with lower characteristic impedance, e.g., 25 Ω, are preferred. Since the cable ends should be put in the climate chamber together with the DUT, where the temperature can be up to 150°C. The insulation materials with higher melting points must be chosen. Since no coaxial connector with 25 Ω is available in the market, the cables are directly mounted to the PCB. Considering the small size of these connection points, the impedance discontinuities caused by
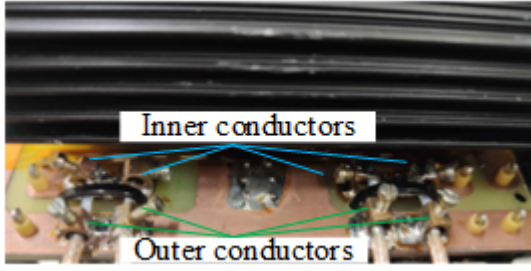
these direct connections can be ignored.
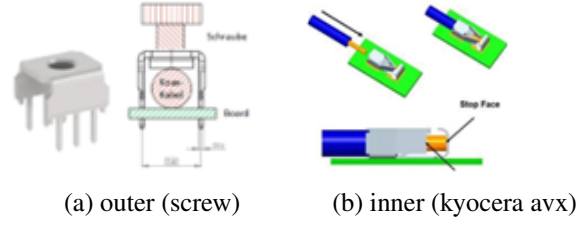

Fig. 11: Screw mounted cables on PCB

(a) outer (screw)　　(b) inner (kyocera avx)

Fig. 12: Alternative connectors

Matching networks

For each 4th order TLT, four resistors of 25 Ω are utilized. They are parallel connected to achieve the required termination resistance and reduce the introduced parasitic inductance. The effective current through each resistor can be derived as:

$$I_R(n.f_s, C_{DUT}) = \frac{1}{n}\sqrt{\frac{3n^3 C_{DUT} V_p^2}{2Z_w T_s} + \frac{2 \cdot t_L}{T_s}\left(\frac{nV_p}{2Z_w}\right)^2} = \frac{V_p}{Z_w}\sqrt{f_s\left(\frac{3n}{2}C_{DUT}Z_w + \frac{t_L}{2}\right)} \tag{8}$$

With a repetition rate of 140 kHz, propagating time of 25 ns, and a load capacitance $C_{DUT} = 64pF$, the calculation yields an RMS current of 0.445 A and power dissipation of 4.95 W in each resistor. It should be noted that current flows through those resistors only before the one-time reflection waves travel back to the line beginning, which lasts $2 \cdot t_L + t_r$ (see Fig.8 (d)).

Ferrite and ferrite sleeves

As already mentioned above, the task of ferrites is to provide sufficient secondary impedance between the outer conductor and the ground. Because different core shapes (ETD, PM, U, and toroid) are used at the same time, the derivation of the mathematical description of this impedance is already beyond the scope of the present work. The optimal number of installed ferrites cannot be estimated analytically, but the criterion is that as long as an improvement of the output waveform could be observed by increasing the number of ferrites, one more ferrite will be added.
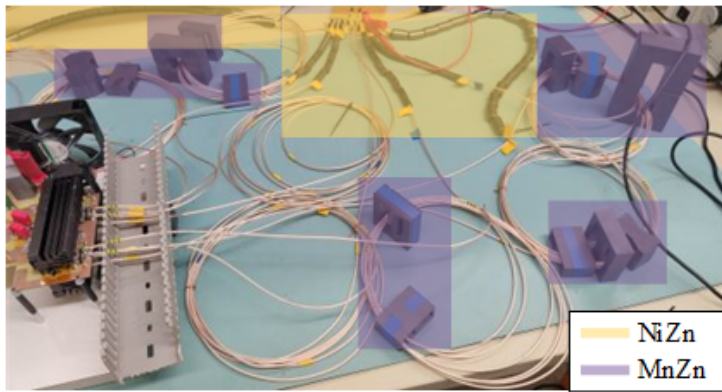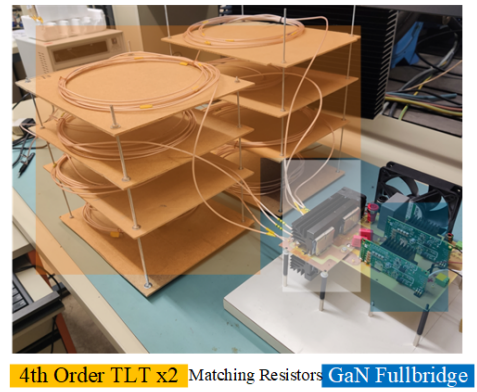

Fig. 13: Ferrites

Fig. 14: Prototype of pulse generator

PCB-Layouts for the full-bridge and impedance matching network

In order to enable an adjustable voltage slew rate, the length of interconnected lines between full-bridge and matching networks can be changed to introduce different values of loop inductance (see Fig.15(c), (d)). The design allows two different ways of connection. With the first variant (c), one can adjust the inductance by using different connection cables, while the smallest loop inductance is achieved via direct connection shown in 15(d).
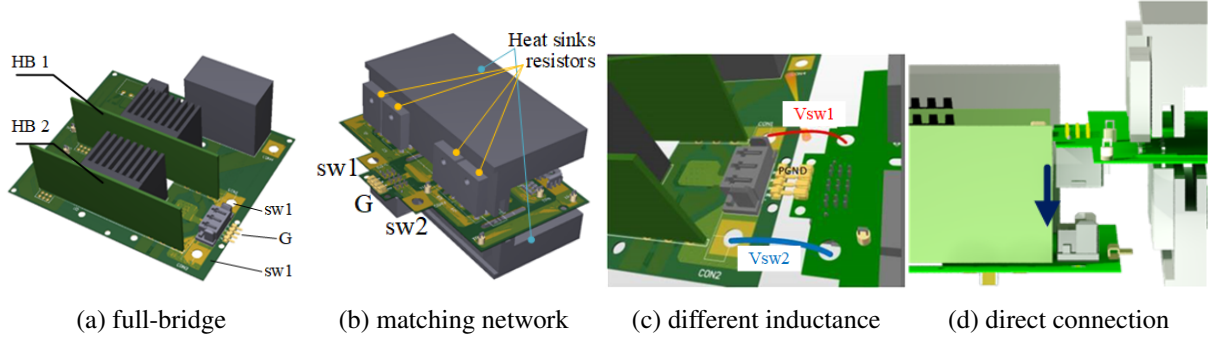
(a) full-bridge   (b) matching network   (c) different inductance   (d) direct connection

Fig. 15: Connection between half-bridges and matching networks

Measuring requirements and experimental results

For the measurement of fast transients or short switching times, an increased bandwidth of the measurement system is required. The lowest bandwidth required to measure a pulse with a rise time, t_r, or a falling time, t_f, can be estimated using the following rule of thumb [14] [16]:

$$BW\ [MHz] = \frac{0.35}{min(t_r, t_f)[ns]} \qquad (9)$$

However, the specification of the bandwidth of a measuring device is usually given in such a way that the measuring signal is already slightly attenuated. Therefore, it is recommended to work with 3-5 times the calculated value. If it is not only about the display of a curve but also about the more precise measurement of the switching times or delay, even 10 times the calculated bandwidth is recommended [14]. For switching times in the 10 ns range, a bandwidth of at least 350 MHz is required.

It is also important to note that the effective bandwidth of the measurement system is determined not only by the oscilloscope but also by the probe used. The approximation of this effective bandwidth can then be made with the following formula:

$$BW_{sys} = \frac{1}{\sqrt{\frac{1}{BW_{osc}^2} + \frac{1}{BW_{probe}^2}}} \qquad (10)$$

Where BW_{sys}, BW_{osc}, and BW_{probe} are the effective bandwidth of the measurement system, the bandwidth of the oscilloscope, and the voltage probe, respectively.

In the presented work, a prototype of the proposed pulse generator with two TLTs of the 4th order is constructed (see Fig.14). In Table I, the selected components for the pulse generator are listed. Forced air is used for the cooling of matching resistors and ferrites. No overheating has been detected during the tests on all components, which ensures a long time operation. Corona discharges were witnessed when the input voltage approached certain voltage values, which depend on the different isolation materials of different DUTs.

Table I: Selected components for the pulse generator

GaN half-bridge	GS66508T-EVBDB2	Ferrites	N87, N97
Coaxial cable	RG316/25 (PTFE), 5 m×8	Ferrite shelves	4W1500
Matching resistor	MP9100-25-1%, thick film		

A maximum voltage slew rate of 249.677 V/ns has been recorded in the measurement with $V_{dc} = 350V$ at no-load condition. It's worth noting that the slew rate during the falling time from 90% to 10% cannot always remain at this maximal value. This slew rate should theoretically be higher at the full voltage of
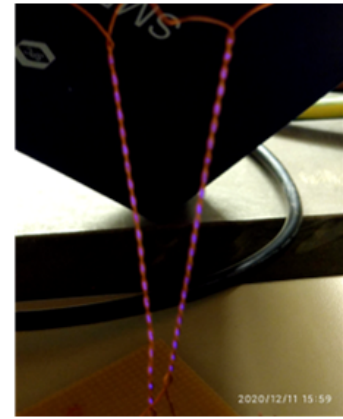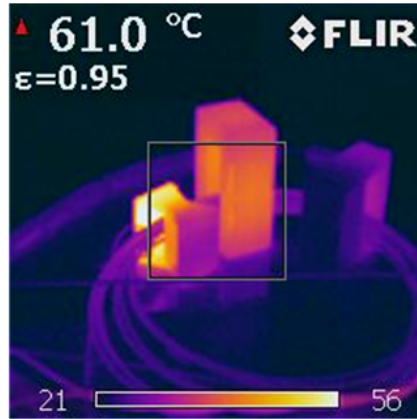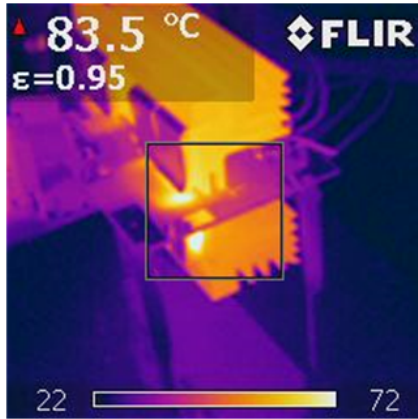
Fig. 16: thermography: resistors (left) ferrites (right)

Fig. 17: Corona discharge

400 V. The dv/dt can be adjusted by changing the DC voltage or the parasitic inductance. As shown in Fig.18, a pulse droop can be observed, and the measured voltage gain at $V_{dc} = 350\,V$ is around 6.8 and lower than the theoretical voltage gain of 8. This can be caused by the loss of TLTs, and the finite large secondary impedance [15], which reduce the lower bandwidth limit of TLTs.
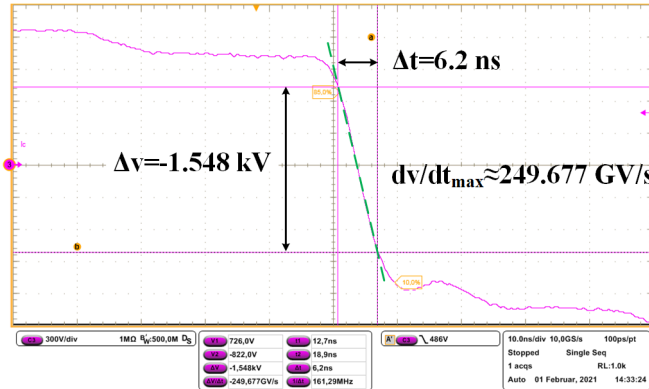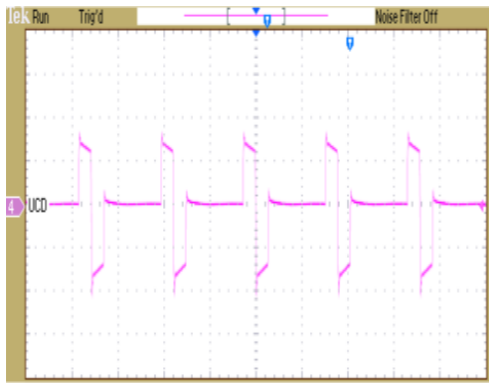

Fig. 18: Output voltage waveform

Fig. 19: Measured maximal voltage slew rate @ $V_{dc} = 350V$

Conclusion

A pulse generator based on TLT and GaN-based full bridge for generating high-repetitive impulse voltage stress with a high slew rate is built and tested. A maximal slew rate of 250 V/ns has been achieved. The generator can be operated at a repetition rate of 140 kHz without problems.

References

[1] GaN-System-Inc.: An Introduction to GaN Enhancement-mode HEMTs, 20 July 2021. [Online] Available: https://gansystems.com/design-center/application-notes/

[2] R. E. Matick:Transmission line pulse transformers—Theory and applications, Proceedings of the IEEE Vol 56 no 1, pp. 47-62, Jan. 1968

[3] W. A. Davis and K. Agarwal: Radio Frequency Circuit Design, John Wiley & Sons, pp. 105-121, 2001

[4] R. A. Mack and J. Sevick: Sevick's Transmission Line Transformers Theory and practice, 5th ed., SciTech Publishing, pp. 3, 2001.

[5] C. Trask: Transmission line transformers: Theory design and applications-part 2, High Frequency Electronics, pp. 46-52, Dec 2005.

[6] K. Yan: Corona plasma generation, Technische Universiteit Eindhoven, 2003.

[7] G. J. J. Winands: Efficient streamer plasma generation, Technische Universiteit Eindhoven, 2007.

[8] J. Horn and G. Boeck: Ultra broadband ferrite transmission line transformer, IEEE MTT-S International Microwave Symposium Digest, pp. 433-436, 15 July 2003.

[9] P. Zacharias: Magnetische Bauelemente, Springer Vieweg, pp. 602-611, 2020.

[10] P. N. Graneau, J. O. Rossi, and P. W. Smith: The operation and modeling of transmission line transformers using a referral method, Review of scientific instruments, pp. 3180-3185, 1999.

[11] TDK: Ferrites and accessories Siferrit material N87, September 2017. [Online] Available: https://www.tdk-electronics.tdk.com/en/529404/products/product-catalog/ferrites-and-accessories/ferrite-materials.

[12] Würth Elektronik: WE-AFB EMI Suppression Axial Ferrite 74270095, [Online] Available: https://www.we-online.com

[13] H. W. Dommel: Digital Computer Solution of Electromagnetic Transients in Single-and Multiphase Networks, IEEE Transactions on Power Apparatus and Systems, pp. 388-399, April 1969.

[14] Tektronix: ABC of the Probes, [Online] Available: https://www.tek.com/en/documents/whitepaper/abcs-probes-primer.

[15] C. Jiang et al.: A compact repetitive nanosecond pulsed power generator based on transmission line transformer, IEEE Transactions on Dielectrics and Electrical Insulation, pp. 1194-1198, 12 August 2011.

[16] Canavero, Flavio G. and Clayton R. Paul: Bandwidth of Digital Waveforms, 2010.